# The role of ATF2 in insulin action

Baan, B.

**Citation**

Baan, B. (2009, June 23). *The role of ATF2 in insulin action*. Retrieved from https://hdl.handle.net/1887/13861

| | |
|---|---|
| Version: | Corrected Publisher's Version |
| License: | [Licence agreement concerning inclusion of doctoral thesis in the Institutional Repository of the University of Leiden](#) |
| Downloaded from: | https://hdl.handle.net/1887/13861 |

**Note:** To cite this publication please use the final published version (if applicable).

# 4

**The role of JNK, p38 and ERK MAP-kinases in insulin-induced Thr69 and Thr71-phosphorylation of transcription factor ATF2**

**Chapter 4**

**Chapter 4**

**The role of JNK, p38 and ERK MAP-kinases in insulin-induced Thr69 and Thr71-phosphorylation of transcription factor ATF2**

Bart Baan, Hans van Dam, Gerard C.M. van der Zon, J. Antonie Maassen
and D. Margriet Ouwens

From the Department of Molecular Cell Biology, Section Signal Transduction and Ageing, Leiden University Medical Centre, Leiden, The Netherlands

**The stimulation of cells with physiological concentrations of insulin induces a variety of responses, like an increase in glucose uptake, induction of glycogen and protein synthesis, and gene expression. One of the determinants regulating insulin-mediated gene expression may be activating transcription factor 2 (ATF2). Insulin activates ATF2 by phosphorylation of Thr69 and Thr71 via a two-step mechanism, in which ATF2-Thr71-phosphorylation precedes the induction of ATF2-Thr69+71-phosphorylation by several minutes. We previously found that in JNK-/- fibroblasts cooperation of the ERK1/2 and p38-pathways is required for two-step ATF2-Thr69+71-phosphorylation in response to growth factors. As JNK is also capable of phosphorylating ATF2, we assessed the involvement of JNK, next to ERK1/2 and p38 in the insulin-induced two-step ATF2-phosphorylation in JNK-expressing A14 fibroblasts and 3T3L1-adipocytes. The induction of ATF2-Thr71-phosphorylation was sensitive to MEK1/2-inhibition with U0126 and this phosphorylation coincided with nuclear translocation of phosphorylated ERK1/2. Use of the JNK-inhibitor SP600125 or expression of dominant negative JNK-activator SEK1 prevented the induction of ATF2-Thr69+71-, but not ATF2-Thr71-phosphorylation by insulin. ATF2-dependent transcription was also sensitive to SP-treatment. Abrogation of p38-activation with SB203580 or expression of dominant negative MKK6 had no inhibitory effect on these events. In agreement with this, the onset of ATF2-Thr69+71-phosphorylation coincided with the nuclear translocation of phosphorylated JNK. Finally, *in vitro* kinase assays using nuclear extracts indicated that ERK1/2-preceded JNK-translocation. We conclude that sequential activation and nuclear appearance of ERK1/2 and JNK rather than p38 underlies the two-step insulin-induced ATF2-phosphorylation in JNK-expressing cells.**

Insulin elicits complex responses in the body in order to maintain glucose and lipid homeostasis. Dependent on the target tissue, insulin regulates a variety of responses, including glucose uptake, glycogen, protein and lipid synthesis and gene expression. Next to the widely studied effects of insulin on the Forkhead/FOXO-transcription factors, also phosphorylation of activating transcription factor 2 (ATF2), may contribute to the effects of insulin on gene expression (1;2).

ATF2 is a ubiquitously expressed member of the cAMP-responsive element (CRE)-binding protein family of basic region-leucine zipper (bZIP) transcription factors also including CREB (3) and ATF3, ATF4, ATF6 and B-ATF (4;5). ATF2 can form homo- and heterodimers with other ATF-family members (5), but also with the activating protein-1 (AP-1) family member cJun (6). The various dimer compositions confer a large repertoire

of target genes on ATF2. Described ATF2 target-genes include cJun, cyclins A and D1, ATF3, Tumor Necrosis Factor α (TNFα) and peroxisome proliferator-activated receptor γ co-activator 1α (PGC1α) (7-13).

In the absence of stimuli, ATF2 is pre-bound to DNA (13;14) and held in an inactive conformation (15). Phosphorylation of residues within the activation domain leads to ATF2 transcriptional activation (16-18). In particular, phosphorylation of two threonine (Thr) residues, Thr69 and Thr71, seems to be required and sufficient for transcriptional activation of ATF2 (7;19).

We previously reported for mouse fibroblasts expressing the human insulin receptor that insulin induces ATF2-activation via phosphorylation of Thr69 and Thr71 via a two-step mechanism (2). Notably, this mechanism involves cooperation of two different pathways. Studies in JNK1,2 -/- embryonic fibroblasts indicated that the ERK1/2-pathway mediates the induction of ATF2-Thr71-phosphorylation, whereas induction of ATF2-Thr69-phosphorylation involves the activity of the p38-pathway (2).

However, JNK is expressed in most cell types and is known to be capable of phosphorylating ATF2 (7;19;20). In addition, purification of endogenous insulin-activated ATF2-kinases identified JNK, next to ERK and p38 as putative candidates (2). These observations prompted us to further determine the contribution of JNK, next to ERK1/2 and p38 in insulin-induced ATF2-phosphorylation in JNK-expressing A14 fibroblasts and 3T3L1 adipocytes. These cell-types were used as representatives of the two major types of insulin-responses: A14 cells respond primarily mitogenic, whereas 3T3L1 adipocytes respond more metabolically to insulin.

We studied *in vivo* and *in vitro* induction of ATF2-Thr71 and ATF2-Th69+71-phosphorylation at various time-points after insulin stimulation using pharmacological inhibitors of the JNK, ERK1/2 and p38-pathways as well as overexpression of dominant negative upstream kinases regulating the activity of JNK and p38. In addition, we examined the insulin-induced nuclear translocation of these kinases by immunofluorescence and assessed nuclear fractions for the presence of *in vitro* nuclear ATF2-kinase activity that could be ascribed to JNK, ERK1/2 or p38.

**Results**

*Differential onset of insulin-induced ATF2-Thr71 and ATF2-Thr69+71-phosphorylation.*
Insulin-treatment of A14 fibroblasts induced the phosphorylation of ATF2 on Thr71 within 2-4 minutes, while phosphorylation of ATF2-Thr69+71 was only achieved at 7-10 minutes after addition of insulin (Figure 1A). A comparable situation was found in 3T3L1 adipocytes, in which insulin-induced ATF2-Thr71–phosphorylation was found after 4 minutes and preceded the induction of ATF2-Thr69+71-phosphorylation (Figure 1B). In contrast, the induction of ATF2-Thr69+71-phosphorylation in response to osmotic shock (O.S.) was not preceded by ATF2-Thr71-phosphorylation (Figure 1C). The induction of ATF2-Thr69+71-phosphorylation was accompanied by a retarded mobility of the protein on ATF2-immunoblot, which was preceded by the induction of an intermediate form after 4 minutes of insulin-treatment (Figure 1D). The induction of this intermediate form coincided with the onset of ATF2-Thr71-phosphorylation and underscores the concept that in response to insulin-treatment the ATF2 protein undergoes a transition from the non-phosphorylated form to the ATF2-Thr69+71-phosphorylated form via an intermediate ATF2-Thr71-phosphorylated form.
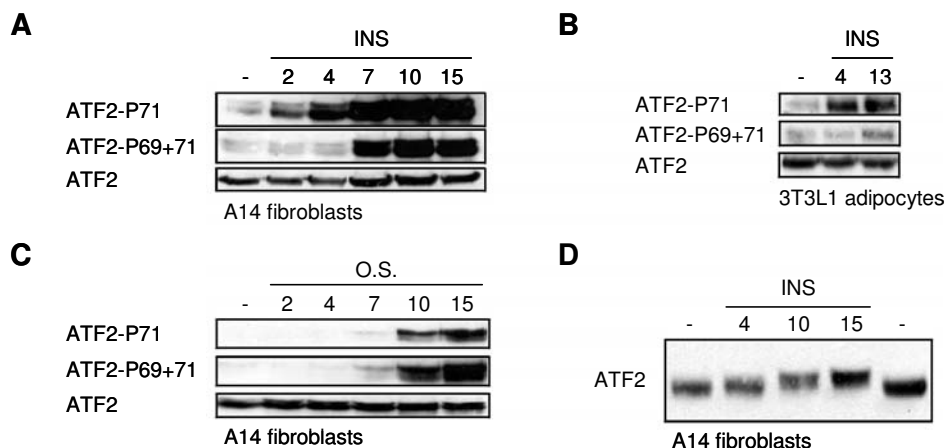
**Figure 1**. Differential onset of insulin-induced ATF2-Thr71 and ATF2-Thr69+71 phosphorylation. Serum-starved A14 cells (A) or 3T3L1 adipocytes (B) were treated with 10 nM insulin (INS). Total cell lysates were prepared at indicated time-points and analyzed by Western blotting using phospho-specific ATF2-Thr71, ATF2-Thr69+71 antibodies. The faster migrating bands recognized by the phospho-specific ATF2-antibodies seem to represent shorter, alternatively spliced, ATF2 products (2). (C) Cell lysates were prepared from A14 cells treated with 0.5 M NaCl (osmotic shock; O.S.) and immunoblotted as described for A and B. (D) Cell lysates prepared from insulin-treated A14 cells as described above were used for extended electrophoresis and subsequently blotted using ATF2-specific antibody.

*Differential onset of insulin-induced MAPK-phosphorylation.*
Upon examining the time-course of ERK1/2, p38 and JNK-activation in A14 fibroblasts, we found that ERK1/2 was phosphorylated within 2 minutes of insulin-treatment (Figure 2A). This phosphorylation was accompanied by *in vitro* ATF2-directed kinase activity in ERK-immunoprecipitates (Figure 2B). Also some phosphorylation of p38 and ATF2-directed kinase activity in p38-immunoprecipitates was observed within 2-4 minutes of insulin-treatment of A14 fibroblasts (Figures 2A and B).
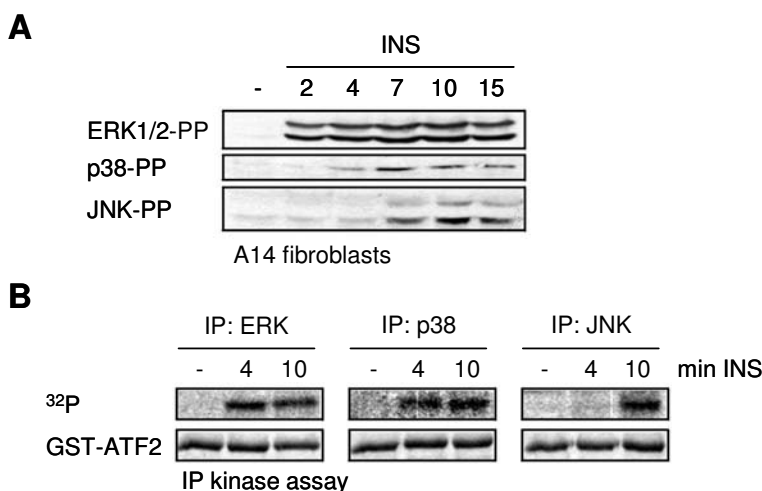


**Figure 2**. Time course of insulin-induced MAPK-phosphorylation. (A) Lysates from serum-starved A14 cells were prepared at the indicated time points after 10 nM insulin-treatment (INS) and were examined for phosphorylation of ERK1/2, p38 and JNK by immunoblotting with phospho-specific antibodies. (B) ERK1/2-, p38- and JNK-immunoprecipitates were analyzed for ATF2-directed kinase activity in an *in vitro* kinase using GST-ATF2 as substrate for 1hr. The Coomassie-stained gel confirmed equal loading of GST-ATF2.

53

The onset of JNK-phosphorylation was delayed compared to ERK- and p38-phosphorylation and was observed after 7 minutes of insulin-treatment. The phosphorylation associated with stimulation of ATF2-kinase activity in JNK-immunoprecipitates (Figure 2A and B).

*Early insulin-induced ATF2-Thr71 phosphorylation is sensitive to inhibition of the MEK-ERK pathway.* As both ERK1/2- and p38-activation coincided with the onset of ATF2-Thr71-phosphorylation, we analyzed the involvement of these MAPKs using pharmacological inhibitors in A14 fibroblasts. Inhibition of p38 using SB203580 (21) had no effect on the induction of ATF2-Thr71 phosphorylation by insulin (Figure 3A). However, prevention of ERK1/2-phosphorylation by the MEK1/2-inhibitor U0126 (22) completely abrogated the induction of ATF2-Thr71 phosphorylation (Figure 3A) and the appearance of the retarded (intermediate) form of ATF2 in response to 4 minutes insulin-treatment (data not shown). Comparable results were obtained in 3T3L1 adipocytes: U0126 prevented insulin-induced increase in ATF2-Thr71-phosphorylation, and pre-treatment with SB203580 had no inhibitory effect on insulin-induced ATF2-Thr71 phosphorylation (Figure 3B).
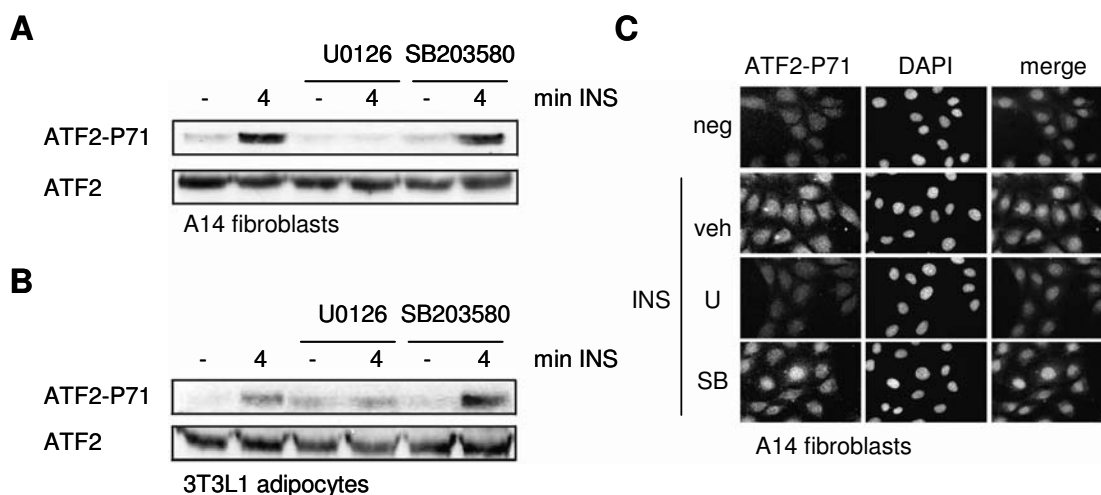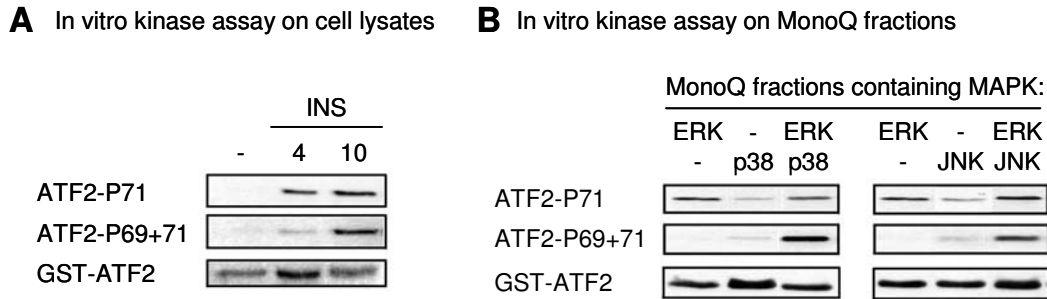


**Figure 3**. Early insulin-induced ATF2-Thr71 phosphorylation is sensitive to inhibition of the MEK1/2-ERK1/2 pathway. Serum-starved A14 cells (A) or 3T3L1 adipocytes (B) were incubated with 10 μM U0126 (U; 15 minutes) or 2.5 μM SB203580 (SB; 30 minutes) before insulin-stimulation (INS; 10 nM) for 4 minutes. Total ATF2 and ATF2-Thr71-phosphorylation levels were determined by immunoblotting with specific antibodies. (C) A14 cells were treated with inhibitors as described above, prior to stimulation with 10 nM of insulin for 4 minutes. Subsequently, cells were fixed and stained with phospho-specific ATF2-Thr71 antibodies followed by FITC-conjugated secondary antibodies (green). DNA was stained with DAPI (blue). Full-colour illustration can be found at page 124.

In line with these data, immunofluorescence experiments on A14 cells demonstrated nuclear phospho-ATF2-Thr71 immunoreactivity detected after 4 minutes of insulin-treatment, which was abolished upon pre-treatment with U0126, but not with SB203580 (Figure 3C). The nuclear localization of ATF2 did not change during the insulin-stimulation (data not shown). Collectively, these results suggest that ERK1/2, rather than p38 is responsible for the insulin-induced phosphorylation of nuclear ATF2 on Thr71 after 4 minutes of stimulation.

*Cooperation of ERK1/2 with p38 or JNK is required for ATF2-Thr69+71-phosphorylation in vitro.* When we analyzed lysates prepared from A14 cells treated for 4 minutes with insulin, predominantly ATF2-Thr71 directed kinase activity was found (Figure 4A). This is in line with the observation that ERK1/2 can only phosphorylate ATF2 on Thr71 and not on Thr69 (2;23). In lysates prepared after 15 minutes of insulin-stimulation, ATF2-Thr71 directed kinase activity was similar to that found in 4 min lysates, but the level of ATF2-Thr69+71 directed kinase activity was markedly increased (Figure 4A). To purify the kinase(s) responsible for the induction of ATF2-Thr69+71 phosphorylation, MonoQ fractionation was performed on lysates prepared after 15 min of insulin stimulation, and the obtained fractions were analyzed for the presence of ATF2-Thr71 directed versus ATF2-Thr69+71 directed kinase activity (2). Approximately 90% of the input ATF2-Thr71 directed kinase activity was recovered after anion-exchange chromatography, and the majority of this fraction (80%) co-purified with fractions, containing ERK1/2 (2). The remaining ATF2-Thr71 directed kinase activity was recovered in fractions co-purifying with JNK and p38 respectively (2). These fractions also contained ATF2-Thr69+71 directed kinase activity. However, in contrast to the almost complete recovery of ATF2-Thr71 directed kinase activity, only 5% of the input ATF2-Thr69+71 directed kinase activity was recovered in the fractions containing JNK and p38 (2). Comparable results were obtained for fractionation of lysates from 3T3L1 adipocytes (data not shown). Collectively, these findings raised the possibility that maximal induction of ATF2-Thr69+71-phosphorylation by insulin requires cooperation of ERK1/2 with p38 and/or JNK. To test this possibility, we added partially purified ERK1/2 to the kinase assays on fractions co-purifying with JNK and p38. Indeed, the weak insulin-induced ATF2-Thr71-directed and Thr69+71-directed kinase-activities co-purifying with p38 and JNK were greatly enhanced by addition of ERK1/2-fraction to the assay (Figure 4B). Similar results were obtained upon addition of recombinant ERK1/2 to the kinase assay (data not shown). Together, these findings suggest that phosphorylation of ATF2 on Thr69 by p38 and/or JNK is more efficient when ATF2 is already phosphorylated on Thr71, at least *in vitro*.

**A** In vitro kinase assay on cell lysates   **B** In vitro kinase assay on MonoQ fractions



**Figure 4**. Cooperation of ERK1/2 with p38 or JNK is required for efficient insulin-induced ATF2-Thr69+71-phosphorylation. (A) Lysates from serum-starved A14 fibroblasts treated with 10 nM insulin (INS) for the indicated times were used in ATF2-directed *in vitro* kinase assays. Site-specific phosphorylation of GST-ATF2 was determined by Western blotting using ATF2-Thr71 and ATF2-Thr69+71 phospho-specific antibodies, respectively. (B) MAPK-containing MonoQ fractions of lysates of 15-minute insulin-treated serum-starved A14 cells were used in *in vitro* ATF2-directed kinase assays for 1hr. Site-specific phosphorylation of GST-ATF2 was determined as described above. Ponceau-staining of the same blot is shown to verify equal loading of GST-ATF2.

*Inhibition of JNK, but not p38, abrogates insulin-induced ATF2-Thr69+71 phosphorylation and activation.* To determine the involvement of p38 and JNK in insulin-induced phosphorylation of ATF2 in intact cells, we used SB203580 and SP600125 (24) to inhibit p38 and JNK, respectively. As shown in Figure 5A and 5B, insulin-induced ATF2-Thr69+71-phosphorylation was abrogated by SP600125, but not SB203580, in both A14 fibroblasts and 3T3L1 adipocytes. Notably, we observed some inhibition of ATF2-Thr71-phosphorylation by SP600125 even under conditions when JNK is not activated, i.e. under basal conditions and at 4 minutes after insulin addition, indicating non-specific side-effects of this inhibitor (Figure 5A). ATF2 band-shift analysis corroborated these results: the slowest migrating (Thr69+71 phosphorylated) form of ATF2 found after 10 minutes was not affected by SB203580, but shifted back to the intermediate form in the presence of SP600125 (Figure 5A).

Similar results were found with the use of dominant negative upstream kinases of p38 and JNK: MKK6-KM and SEK1-KR, respectively (see Figure 5C): Overexpression of SEK1-KR abrogated only the insulin-induced ATF2-Thr69+71 phosphorylation but not the Thr71-phosphorylation found after 15 minutes of insulin-stimulation. Overexpression of MKK6-KM had no effect on insulin-induced ATF2-phosphorylation (Figure 5C).
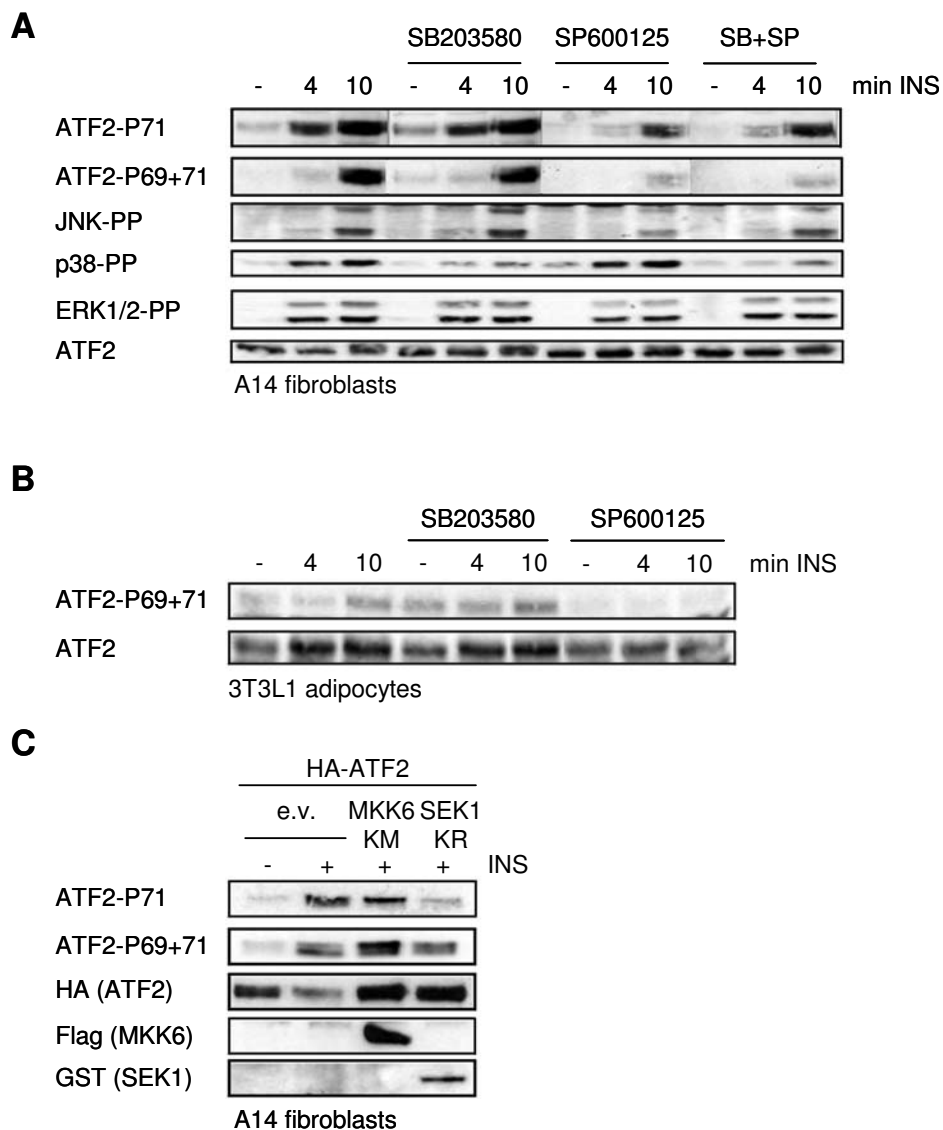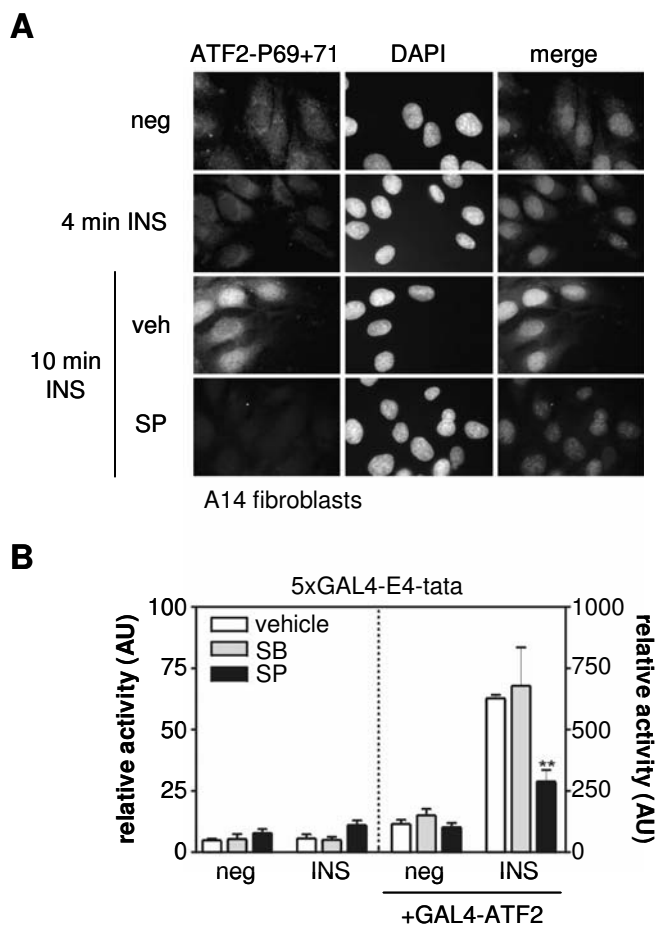
**Figure 5.** Inhibition of JNK, but not p38, abrogates insulin-induced ATF2-Thr69+71 phosphorylation. Serum-starved A14 fibroblasts (A) or 3T3L1 adipocytes (B) were incubated for 30 minutes with DMSO, 2.5 µM SB203580 (SB), 10 µM SP600125 (SP) or SB+SP prior to stimulation with 10 nM insulin (INS) for the indicated times. Phosphorylation of ATF2-Thr71, ATF2-Thr69+71, JNK, p38 and ERK1/2 was determined with phospho-specific antibodies. (C) A14 fibroblasts were transfected with either an empty vector (e.v.) or expression vectors for epitope-tagged dominant negative MKK6-KM or SEK1-KR together with pBabe-puro and pMT2-HA-ATF2. Puromycin-resistant cells were selected, serum-starved overnight and subsequently stimulated with 10 nM insulin for 15 minutes. Phosphorylation of ATF2-Thr71, ATF2-Thr69+71 was determined with phospho-specific antibodies.

Immunofluorescence experiments showed that 10 minutes of insulin-treatment increased nuclear ATF2-Thr69+71 immunoreactivity compared to 4 minutes and untreated A14 cells, and that this immunoreactivity was sensitive to SP600125 (Figure 6A).

To determine whether modulation of insulin-induced ATF2-Thr69+71-phosphorylation affected ATF2-mediated transcription accordingly, we examined the insulin-induced activation of a GAL4-ATF2-dependent luciferase reporter. Insulin-induced activation was significantly inhibited by SP600125 (P=0.0097), but not by SB203580 (Figure 6B).



**Figure 6**. Inhibition of JNK, but not p38, abrogates the insulin-induced ATF2-phosphorylation and activation. (A) Serum-starved A14 cells were treated with inhibitors as described above prior to stimulation with 10 nM insulin (INS) for the indicated times. Cells were fixed and stained with antibodies for Thr69+71-phosphorylated ATF2 followed by FITC-conjugated secondary antibodies (green). DNA was stained with DAPI (blue). (B) Insulin-induced ATF2 transcriptional activity was examined in a GAL4-dependent luciferase reporter assay using the activation domain of ATF2 fused to the GAL4 DNA binding domain (19). Cells were transiently transfected and grown for 8 hours, subsequently serum-starved in DMEM containing 0.5% FBS O/N and treated for 30 minutes with vehicle or inhibitors SB203580 or SP600125 before adding insulin (INS; 10 nM). Cells were lysed 16 hrs later and luciferase activity was determined. The relative firefly luciferase activity is depicted as the mean enhancement of promoter activity in the absence or presence of insulin and/or inhibitors +/- the SD of three independent experiments performed in triplicates. Note the different scaling of the left and right *y*-axis. ** *P* = 0.0097 in a Student t-test. Full-colour illustration can be found at page 125.

*The onset of ATF2-Thr71 and ATF2-Thr69+71-phosphorylation associates with nuclear translocation of ERK1/2 and JNK.* The experiments described above suggest that cooperation of ERK1/2 with JNK, rather than with p38, is required for insulin-induced two-step ATF2-Thr69+71-phosphorylation. To corroborate these findings we examined whether ERK1/2 and JNK translocate to the nucleus in response to insulin. We found that within 4 minutes, insulin induced the phosphorylation and nuclear translocation of ERK1/2 (ERK1/2-PP; See Figure 7A). U0126 pre-treatment strongly inhibited the ERK1/2-PP signal and reduced nuclear staining found with a pan-ERK1/2 antibody (Figure 7A and data not shown).
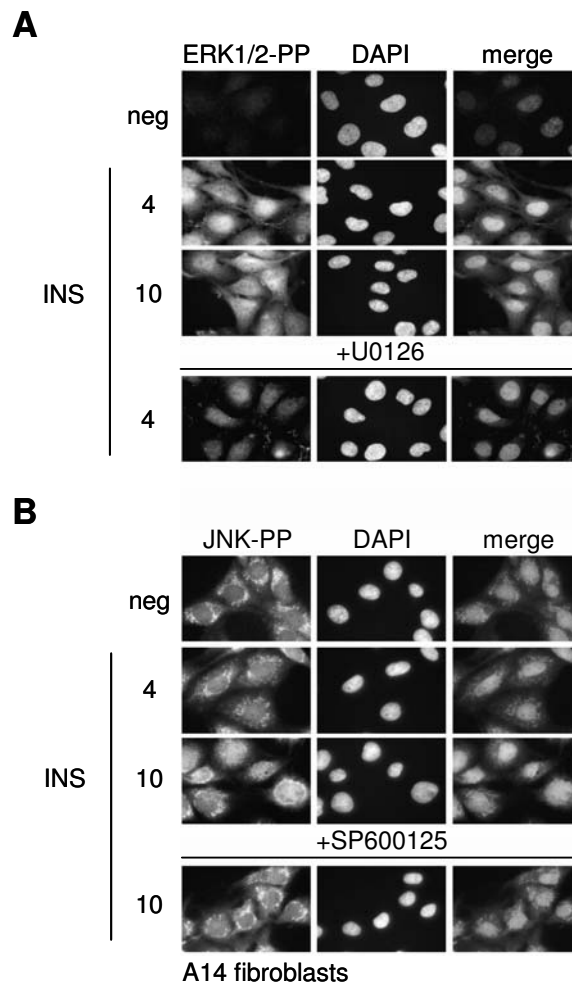


**Figure 7**. Time course of nuclear translocation of ERK1/2 and JNK. Serum-starved A14 cells were incubated with DMSO, 10 μM U0126 (U) for 15 minutes or 10 μM SP600125 (SP) for 30 minutes prior to stimulation with 10 nM insulin (INS) for the indicated times. Cells were fixed and stained with antibodies for (A) phosphorylated ERK (ERK-PP) or (B) phosphorylated JNK (JNK-PP) and FITC-conjugated secondary antibodies (green). DNA was stained with DAPI (blue). Full-colour illustration can be found at page 126.

Despite the high a-specific background-level of (non-nuclear) phosphorylated JNK (JNK-PP)-signal in the absence of insulin, no increase in JNK-PP staining could be detected after 4 minutes of insulin-treatment (Figure 7B). The amount of JNK-PP in the nucleus was substantially increased after 10 minutes of insulin-stimulation and this response was inhibited by SP600125 (Figure 7B).

In line with the immunofluorescence data, we found that nuclear extracts prepared from cells after 4 minutes of insulin stimulation contained predominantly ATF2-Thr71-directed kinase activity (Figure 8A). This ATF2-Thr71-directed activity could be abrogated by addition of ERK-inhibitor 5-iodotubercidin (Itu (25)) and was absent in nuclear extracts from U0126-treated cells (data not shown). The ATF2-Thr71-directed kinase activity in these nuclear extracts was not affected by SP600125 or SB203580 (Figure 8A).

Nuclear extracts obtained after 10 minutes of insulin-stimulation contained both ATF2-Thr71- and ATF2-Thr69+71-directed kinase activity (Figure 8B). Addition of the JNK-inhibitor SP600125 only abrogated the ATF2-Thr69+71-phosphorylation, but not the ATF2-Thr71-directed activity (Figure 8B). SB203580 did not affect the ATF2-Thr69+71 and ATF2-Thr71 activities, whereas Itu reduced both ATF2-Thr71- and ATF2-Thr69+71 kinase activities.
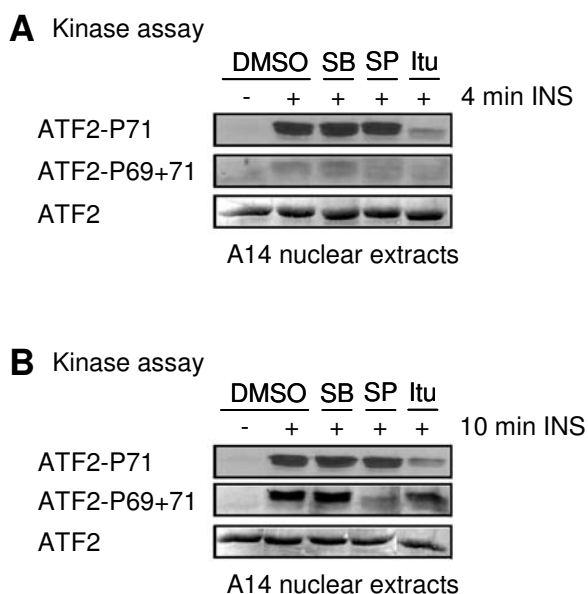


**Figure 8**. Sequential appearance of ERK1/2- and JNK-dependent ATF2-directed nuclear kinase activities. Serum-starved A14 cells stimulated with 10 nM insulin for 4 minutes (A) or 10 minutes (B). Nuclear proteins were extracted and used in *in vitro* ATF2-directed kinase assays for 2 hrs in the presence of DMSO or inhibitors 2.5 μM SB203580 (SB), 5 μM SP600125 (SP) or 5 μM 5-iodotubercidin (Itu). Site-specific phosphorylation of GST-ATF2 was determined by Western blotting using ATF2-Thr71 and ATF2-Thr69+71 phospho-specific antibodies. Ponceau-staining of the same blot is shown to verify of equal loading of GST-ATF2.

## Discussion

The present study addresses the activation of the transcription factor ATF2 by insulin. It extends our previous findings (2) by addressing the mechanism via which insulin accomplishes this activation in A14 cells and 3T3L1 adipocytes. The results of this study suggest the following model for the induction of ATF2-Thr69+71 phosphorylation in response to insulin (summarized in Figure 9): within 2-4 minutes, insulin induces activation of ERK1/2, which translocates to the nucleus and mediates ATF2-Thr71-phosphorylation. Between 5-10 minutes after the addition of insulin, JNK is activated, translocates to the nucleus and mediates Thr69-phosphorylation of phospho-Thr71-ATF2, thereby activating the transcription factor. We propose that the sequential activation and subsequent nuclear appearance of ERK1/2 and JNK are rate limiting for the two-step phosphorylation of ATF2-Thr69+71 in response to insulin.

Previously, we reported that in JNK-/- cells, the ERK1/2- and the p38-pathways cooperate in the growth factor-induced phosphorylation of ATF2-Thr69+71 (2). Although this study indicates that JNK may be dispensable for insulin-mediated ATF2-phosphorylation, pharmacological inhibition of p38 in JNK-expressing cells had no inhibitory effect on the induction ATF2-phosphorylation, suggesting that JNK rather than p38 regulates this response.

Accordingly, various studies have identified JNK as a bona fide ATF2-kinase (2;7;19;20;23). An important finding of the present study, however, is that JNK predominantly functions as ATF2-Thr69-kinase for ATF2 already phosphorylated on Thr71, in the proposed two-step ATF2-Thr69+71 phosphorylation-mechanism induced by insulin. In contrast, in response to inducers of cellular stress like UV, methyl methane sulphonate (MMS), osmotic shock and TNFα, the onset of ATF2-Thr69+71 coincides with the onset of ATF2-Thr71-phosphorylation, and this process seems completely JNK-dependent in JNK-expressing cells (2;7;23 and data not shown).
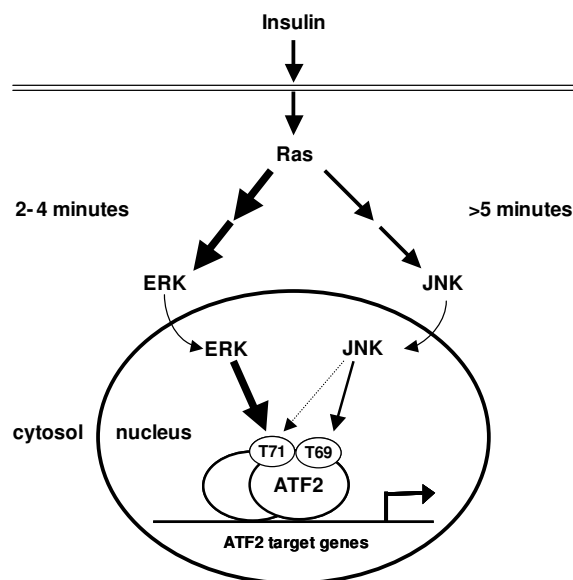


**Figure 9**. Proposed model for insulin-induced ATF2-activation in A14 cells and 3T3L1 adipocytes. Insulin induces activation of ERK1/2 within 2-4 minutes. ERK1/2 subsequently translocates to the nucleus, where it mediates ATF2-Thr71-phosphorylation. Subsequently JNK is activated, translocates to the nucleus and efficiently phosphorylates Thr71-phosphorylated ATF2 on Thr69, thus inducing transcriptional activation of ATF2.

This raises the question whether activation of JNK alone may be sufficient for the induction of ATF2-phosphorylation in response to insulin-treatment. However, the data shown here are indicative that also ERK1/2 activation seems to biologically relevant for insulin-mediated two-step ATF2-phosphorylation. Biochemical evidence for its involvement is provided by changes in electrophoretic mobility of the ATF2 protein during the course of insulin-mediated phosphorylation. After insulin stimulation, the ATF2-protein undergoes a transition via an ATF2-Thr71 phosphorylated form to an ATF2-Thr69+71 phosphorylated form. More importantly, pharmacological inhibition of ERK-activation prevented early ATF2-Thr71 phosphorylation and the accompanying retarded mobility of the protein. In addition, ERK1/2- and ATF2-Thr71-phosphorylation are found several minutes before JNK-activation and ATF2-Thr69+71 phosphorylation were detectable. Collectively, these findings highlight the importance of ERK1/2 for insulin-induced ATF2-phosphorylation and provide support for our model.

We and others have demonstrated that ERK preferentially phosphorylates ATF2 on Thr71, whereas the kinase seems incapable to efficiently mediate ATF2-Thr69 phosphorylation (2;23). Therefore, cooperation with another kinase seems required for induction of ATF2-Thr69+71 phosphorylation in response to insulin. Interestingly, while MonoQ fractionation of lysates from osmotic-shock treated cells yielded similar recoveries for ATF2-Thr69+71 and ATF2-Thr71 directed kinase activities, in cell extracts from insulin-treated cells, only ~5% of the ATF2-Thr69+71 directed *in vitro* kinase activity was recovered, in contrast to ~80% recovery of ATF2-Thr71 directed activity (for details see reference (2)) Importantly, the weak insulin-induced ATF2-Thr69+71 kinase activities, which co-purified with JNK and p38 respectively, were greatly enhanced by the addition of ERK1/2 to the kinase reaction. Collectively, these findings strongly suggest that insulin-activated MAP kinases cooperate to induce efficient ATF2-Thr69+71 phosphorylation and provide strong support for our two-step model.

Previously, Waas and coworkers (26) found that recombinant active p38 phosphorylates GST-ATF2 via a two-step (double collision) mechanism, involving the dissociation of mono-phosphorylated Thr71-ATF2 or Thr69-ATF2 from the enzyme after the first phosphorylation step. Importantly, these authors found that mono-phosphorylation of ATF2-Thr69 strongly reduces the phosphorylation rate of Thr71, whereas, mono-phosphorylation of Thr71 does not reduce the rate of Thr69 phosphorylation (26). Thus, efficient phosphorylation of ATF2 by recombinant active p38 only occurs in the order Thr71 → Thr69+71. In our model, phosphorylation of ATF2-Thr71 by ERK1/2 might prime ATF2 for subsequent efficient ATF2-Thr69-phosphorylation. As described above, the kinase assays on MonoQ fractions indicate that both p38 and JNK can indeed enhance the phosphorylation of ATF2-Thr69+71 in the presence of activated ERK1/2 *in vitro*. In cultured cell lines expressing both kinases, however, JNK rather than p38 seems to mediate this second phosphorylation. Several lines of evidence point in this direction: First, chemical inhibition of JNK-activity with SP600125, or prevention of JNK-activation by overexpression of dominant negative SEK1 abrogated only the Thr69+71-phosphorylation in response to insulin. Second, prevention of p38-activation by overexpression of dominant negative MKK6 or inhibition of p38 by SB203580 failed to affect insulin-mediated ATF2-phosphorylation in JNK-expressing cells. In part, the absence of the inhibitory effect of SB could be ascribed to an enhanced activation of JNK which was observed in the presence of this inhibitor ((2) see also Figure 5 and Supplementary Figure S1). However, simultaneous addition of SB203580 and SP600125 had the same effect as SP600125 alone, suggesting

that this is not the case. In addition, we could not obtain evidence for nuclear translocation of activated p38 in insulin-treated cells neither in immunofluorescence assays nor in *in vitro* kinase assays on nuclear extracts.

To exclude the possibility that SB203580 was unable to inhibit p38, we analyzed inhibition of p38-activity by SB203580 *in vitro* and *in vivo*. In *in vitro* kinase assays the SB-compound completely abrogated ATF2-directed kinase activity found in p38-containing MonoQ-fractions of insulin-stimulated A14 fibroblasts (data not shown). Also, we found that phosphorylation of p38's downstream nuclear target MAPKAPK2 (MK2 (27)) in response to insulin in JNK-/- cells was sensitive to SB203580-treatment (data not shown). Interestingly, although in A14 fibroblasts p38-activity was induced by insulin and reduced by SB203580-treatment, no MK2-phosphorylation could be detected in these cells (Figure S1). In contrast, O.S. did induce robust phosphorylation of both p38 and MK2, which were reduced and abrogated, respectively by SB203580-treatment (Figure S1). These observations suggest that the SB203580-compound was functional in *in vitro* and *in vivo* assays. In addition, it seems that in JNK-containing A14 cells, insulin-induced phospho-p38 is confined to the cytosol or does not reach its nuclear target MK2, while it does after O.S.-stimulation.

Collectively, these data support the idea that JNK rather than p38 is responsible for the second phosphorylation event, and that p38 seems only capable of inducing ATF2-phosphorylation under conditions that JNK is genetically absent.

**Materials and Methods**

*Cell culture and cell stimulation.* A14 cells (NIH 3T3 fibroblasts overexpressing the human insulin receptor (28)) were cultured in Dulbecco's modified Eagle's medium (DMEM) containing 9% fetal bovine serum (FBS) and antibiotics. 3T3L1 fibroblasts were obtained from ATCC and differentiated to adipocytes as described (29). Briefly, 3T3L1 cells were grown to confluence. Two days post-confluence, differentiation was induced by culturing cells for 2 days on DMEM/FBS supplemented with 10 µg/ml of bovine insulin (Sigma), 0.25 µM dexamethasone (Sigma) and 0.5 mM 3-isobutyl-1-methylxanthine (Sigma), followed by DMEM/FBS containing only insulin (10 µg/ml). Differentiated adipocytes were maintained for another 6 days in DMEM/FBS prior to use. Before cell-stimulations, the cells were serum-starved (DMEM w/ 0.5% FBS) for 16h. When inhibitors were used, cells were pre-treated for 30 minutes with 10 µM SP600125 (Biomol) or 2.5 µM SB203580 (Promega) or for 15 minutes with 10 µM U0126 (Promega), before addition of bovine insulin to 10 nM or NaCl (osmotic stress; O.S.) to 500 mM.

*Transient transfection and luciferase assays.* For overexpression experiments, A14 cells were co-transfected in 6 well plates with a total of 1.5 µg of DNA per well; 0.875 µg of either a carrier vector or expression vectors encoding epitope-tagged dominant negative MKK6-K82M or SEK1-K129R (kindly provided by Dr J. Kyriakis), 0.5 µg pMT2-HA-ATF2 (2) and 0.125 µg pBabe-puro using FUGENE6 transfection reagent (Roche) according to suppliers protocol. Cells were selected with 3 µg/ml of puromycin (Sigma) for 3-5 days, after which cells were serum-starved overnight, stimulated with 10 nM insulin for 15 minutes and lysed and blotted as described above.

For GAL4-luciferase assays, A14 cells were transfected in 6 well plates using the DEAE–dextran method as described (30). For each well 0.25 µg pGl3-GAL4-E4-luciferase reporter (2) was co-transfected with 1 µg of carrier vector psp64 and 1 µg of either pC2-Gal4-ATF2-TAD (19) or the carrier vector. Briefly, DNA was mixed in 1 mg/ml DEAE-

dextran-supplemented TBS [25 mM Tris; pH 7.4, 150 mM NaCl, 5 mM KCl, 0.7 mM CaCl$_2$ and 0.5 mM MgCl$_2$] and added to cells. After a 30-minute incubation, cells were washed and DMEM/FBS was added. After 8 hours, cells were serum-starved in DMEM containing 0.5% FBS and 24 hours after transfection cells were pre-treated with inhibitors before adding insulin (to 10 nM). 16 hours later, cells were lysed in luciferase lysis buffer [25 mM Tris, pH 7.8, 2 mM dithiotreitol, 2 mM 1,2-diaminocyclohexane-*N,N,N',N'*-tetraacetic acid, 10% glycerol and 1% Triton X-100] and luciferase activity was determined according to the manufacturer's protocol (Promega).

*Western blot analysis and antibodies.* Whole cell lysates were prepared from 9 cm dishes that were rinsed twice with ice-cold phosphate-buffered saline (PBS) and lysed in 750 µl Laemmli sample buffer. Proteins were separated on polyacrylamide slab gels and transferred to Immobilon (Millipore). Blots were stained with Ponceau S before blocking to verify equal loading and appropriate protein transfer. Filters were incubated with antibodies as described previously (2). The antibodies used were: Lamin A and phospho-specific ATF2-Thr69+71, ATF2-Thr71, p38-Thr180/Tyr182, ERK1/2-Thr202/Tyr204 (all polyclonal) and JNK-Thr183/Tyr185 monoclonal (all from Cell Signaling Technology); p38 (N-20), ATF2 (C-19) and ERK1 (K-23) (Santa Cruz) and secondary antibodies: goat anti-rabbit and goat anti-mouse IgG–HRP conjugate (Promega). The total JNK and EF-1β antibodies were described previously (2;31). For ATF2 band shift analysis, immunoblots were prepared after separation of proteins on large 7% polyacrylamide slab gels, and incubated with ATF2 (C-19) antibody.

*MonoQ/anion-exchange chromatography.* Anion-exchange chromatography was performed essentially as described previously (2). Briefly, stimulated cells were scraped in MonoQ lysis buffer [20 mM Tris (pH 7.0), 0.27 M sucrose, 1 mM EDTA, 1 mM EGTA, 1% Triton X-100, 10 mM sodium β-glycerolphosphate, 50 mM NaF, 5 mM sodium pyrophosphate, 1 mM sodium orthovanadate, 0.1% (v/v) β-mercaptoethanol and Complete protease inhibitors (Roche Biochemicals)]. Lysates of six 9-cm dishes (~8000 mg protein) were diluted twofold with MonoQ buffer [50 mM Tris.Cl (pH 7.5), 1 mM EDTA, 1 mM EGTA, 5% (v/v) glycerol, 0.03% (w/v) Brij-35, 1 mM benzamidine, 0.3 mM sodium orthovanadate, and 0.1% (v/v) β-mercaptoethanol] and applied to a MonoQ HR 5/5 column (Amersham Pharmacia Biotech) equilibrated in MonoQ buffer. After washing, the column was developed with a linear salt gradient to 700 mM NaCl in MonoQ buffer and fractions of 1 ml were collected. Aliquots of 10 µl from each fraction were used in *in vitro* ATF2 kinase assays.

*Preparation of nuclear extracts.* For extraction of nuclear proteins, cell lysates were prepared from 9 cm dishes that were rinsed twice with ice-cold phosphate buffered saline (PBS) and scraped in 1 ml of cold RIPA buffer [30 mM Tris–HCl pH 7.5, 1mM EDTA, 150 mM NaCl, 0.5% Triton X-100, 0.5% Na-DOC, 1 mM sodium orthovanadate, 10 mM sodium fluoride and Complete protease inhibitors (Roche)]. Nuclei were pelleted by centrifugation (10 min, 14000 rpm, 4°C). Supernatants were collected and stored as cytosolic fractions. Nuclear pellets were washed twice with RIPA and were then incubated on ice for 1hr with 75 µl of extraction buffer [30 mM Tris-HCl pH 7.5, 300 mM NaCl, 1 mM EDTA with Complete protease inhibitors (Roche)] and vortexed every 5 min. After centrifugation, supernatants were collected and used as nuclear protein extracts. Protein content was determined using the BCA-kit (Pierce). Purity of the cell fractions was checked by Western Blotting, using EF-1β and Lamin A antibodies as cytosolic and nuclear markers, respectively (see supplementary Figure S2).

*ATF2 kinase assays.* For *in vitro* ATF2 kinase assays, equal volumes of MonoQ-fractions and equal amounts of protein from cytosolic or nuclear extracts were incubated at 30°C with 2 μg of purified GST-ATF2-N substrate (7) and 50 μM ATP in a total volume of 60 μl of kinase buffer [25 mM HEPES, pH 7.4, 25 mM MgCl2, 25 mM β-glycerolphosphate, 5 mM β-mercaptoethanol and 100 μM sodium orthovanadate]. When indicated, kinase assays were performed in the presence of vehicle (DMSO) or inhibitors SB203580 (2.5 μM), SP600125 (5 μM) or iodotubercidin (Itu;5 μM (25)). Reactions were terminated by the addition of 20 μl of 4x Laemmli buffer and subsequently analyzed by SDS–PAGE/immunoblotting with phospho-specific ATF2-Thr69+71 and ATF2-Thr71 antibodies. The specificity of these antibodies has been verified previously (2;23).

For immunoprecipitation kinase assays, RIPA cell lysates were prepared as described above and equal aliquots (750 μg) were nutated overnight with 10 μl of p38, JNK, or ERK antibodies coupled to protein A-sepharose beads (Pharmacia) at 4°C. The antibodies used for immunoprecipitation were: ERK 2199 (32), p38 N20 (Santa Cruz) and JNK1 FL (Santa Cruz). Beads were collected by centrifugation and were washed four times with RIPA buffer, and two times with kinase buffer. Subsequently, the beads were incubated with 2 μg of purified GST-ATF2-N substrate (7) and 50 μM ATP, containing 2 μCi [γ-$^{32}$P]ATP, in a total volume of 60 μl of kinase buffer for 1 at 30°C.

*Immunofluorescence.* Cells were grown on coverslips. After stimulation, cells were washed twice with ice-cold PBS and subsequently fixed in 3.7% formaldehyde in PBS for 15 minutes at room temperature. Coverslips were washed with Tris buffered saline [TBS; 25 mM Tris, 100 mM NaCl, 5 mM KCl, 0.7 mM CaCl$_2$.2H$_2$O, 0.5 MgCl$_2$.6H2O] and permeabilised for 5 minutes with 0.1% Triton X-100 in TBS, subsequently washed with 0.2% BSA/TBS, blocked for 30 minutes in 2% BSA/TBS at room temperature and then incubated overnight at 4°C with primary antibodies diluted 1:250 in 0.2% BSA/TBS. After 0.2% BSA/TBS washes, coverslips were incubated with appropriate secondary antibodies diluted 1:100 in 0.2% BSA/TBS for 2 hrs at room temperature. Thereafter coverslips were washed sequentially with 0.2% BSA/TBS and TBS, mounted in DAPI-containing Vectashield solution (Vector Laboratories) and fixed with nail polish. Fluorescence was detected using a Leica DM-RXA microscope. Pictures were acquired as color images (MERGE) and prepared using Photopaint and Coreldraw software.

**References**
1. Accili D, Arden KC 2004 FoxOs at the crossroads of cellular metabolism, differentiation, and transformation. Cell 117:421-426
2. Ouwens DM, De Ruiter ND, Van Der Zon GC, Carter AP, Schouten J, Van Der Burgt C, Kooistra K, Bos JL, Maassen JA, van Dam H 2002 Growth factors can activate ATF2 via a two-step mechanism: phosphorylation of Thr71 through the Ras-MEK-ERK pathway and of Thr69 through RalGDS-Src-p38. EMBO J 21:3782-3793
3. Mayr B, Montminy M 2001 Transcriptional regulation by the phosphorylation-dependent factor CREB. Nat Rev Mol Cell Biol 2:599-609
4. Hai T, Hartman MG 2001 The molecular biology and nomenclature of the activating transcription factor/cAMP responsive element binding family of transcription factors: activating transcription factor proteins and homeostasis. Gene 273:1-11
5. Hai TW, Liu F, Coukos WJ, Green MR 1989 Transcription factor ATF cDNA clones: an extensive family of leucine zipper proteins able to selectively form DNA-binding heterodimers. Genes Dev 3:2083-2090

6. Hai T, Curran T 1991 Cross-family dimerization of transcription factors Fos/Jun and ATF/CREB alters DNA binding specificity. Proc Natl Acad Sci USA 88:3720-3724
7. van Dam H, Wilhelm D, Herr I, Steffen A, Herrlich P, Angel P 1995 ATF-2 is preferentially activated by stress-activated protein kinases to mediate c-jun induction in response to genotoxic agents. EMBO J 14:1798-1811
8. Shimizu M, Nomura Y, Suzuki H, Ichikawa E, Takeuchi A, Suzuki M, Nakamura T, Nakajima T, Oda K 1998 Activation of the rat cyclin A promoter by ATF2 and Jun family members and its suppression by ATF4. Exp Cell Res 239:93-103
9. Beier F, Lee RJ, Taylor AC, Pestell RG, LuValle P 1999 Identification of the cyclin D1 gene as a target of activating transcription factor 2 in chondrocytes. Proc Natl Acad Sci U S A 96:1433-1438
10. Kool J, Hamdi M, Cornelissen-Steijger P, van der Eb AJ, Terleth C, van Dam H 2003 Induction of ATF3 by ionizing radiation is mediated via a signaling pathway that includes ATM, Nibrin1, stress-induced MAPkinases and ATF-2. Oncogene 22:4235-4242
11. Tsai EY, Jain J, Pesavento PA, Rao A, Goldfeld AE 1996 Tumor necrosis factor alpha gene regulation in activated T cells involves ATF-2/Jun and NFATp. Mol Cell Biol 16:459-467
12. Cao W, Daniel KW, Robidoux J, Puigserver P, Medvedev AV, Bai X, Floering LM, Spiegelman BM, Collins S 2004 p38 Mitogen-Activated Protein Kinase Is the Central Regulator of Cyclic AMP-Dependent Transcription of the Brown Fat Uncoupling Protein 1 Gene. Mol Cell Biol 24:3057-3067
13. Hayakawa J, Mittal S, Wang Y, Korkmaz KS, Adamson E, English C, Omichi M, McClelland M, Mercola D 2004 Identification of Promoters Bound by c-Jun/ATF2 during Rapid Large-Scale Gene Activation following Genotoxic Stress. Mol Cell 16:521-535
14. Herr I, van Dam H, Angel P 1994 Binding of promoter-associated AP-1 is not altered during induction and subsequent repression of the c-jun promoter by TPA and UV irradiation. Carcinogenesis 15:1105-1113
15. Li XY, Green MR 1996 Intramolecular inhibition of activating transcription factor-2 function by its DNA-binding domain. Genes Dev 10:517-527
16. Sakurai A, Maekawa T, Sudo T, Ishii S, Kishimoto A 1991 Phosphorylation of cAMP response element-binding protein, CRE-BP1, by cAMP-dependent protein kinase and protein kinase C. Biochem Biophys Res Commun 181:629-635
17. Sevilla A, Santos CR, Vega FM, Lazo PA 2004 Human vaccinia-related kinase 1 (VRK1) activates the ATF2 transcriptional activity by novel phosphorylation on Thr-73 and Ser-62 and cooperates with JNK. J Biol Chem 279:27458-27465
18. Ban N, Yamada Y, Someya Y, Ihara Y, Adachi T, Kubota A, Watanabe R, Kuroe A, Inada A, Miyawaki K, Sunaga Y, Shen ZP, Iwakura T, Tsukiyama K, Toyokuni S, Tsuda K, Seino Y 2000 Activating transcription factor-2 is a positive regulator in CaM kinase IV-induced human insulin gene expression. Diabetes 49:1142-1148
19. Livingstone C, Patel G, Jones N 1995 ATF-2 contains a phosphorylation-dependent transcriptional activation domain. EMBO J 14:1785-1797
20. Gupta S, Campbell D, Derijard B, Davis RJ 1995 Transcription factor ATF2 regulation by the JNK signal transduction pathway. Science 267:389-393

21. Cuenda A, Rouse J, Doza YN, Meier R, Cohen P, Gallagher TF, Young PR, Lee JC 1995 SB 203580 is a specific inhibitor of a MAP kinase homologue which is stimulated by cellular stresses and interleukin-1. FEBS Lett 364:229-233

22. Favata MF, Horiuchi KY, Manos EJ, Daulerio AJ, Stradley DA, Feeser WS, Van Dyk DE, Pitts WJ, Earl RA, Hobbs F, Copeland RA, Magolda RL, Scherle PA, Trzaskos JM 1998 Identification of a novel inhibitor of mitogen-activated protein kinase kinase. J Biol Chem 273:18623-18632

23. Morton S, Davis RJ, Cohen P 2004 Signalling pathways involved in multisite phosphorylation of the transcription factor ATF-2. FEBS Lett 572:177-183

24. Bennett BL, Sasaki DT, Murray BW, O'Leary EC, Sakata ST, Xu W, Leisten JC, Motiwala A, Pierce S, Satoh Y, Bhagwat SS, Manning AM, Anderson DW 2001 SP600125, an anthrapyrazolone inhibitor of Jun N-terminal kinase. Proc Natl Acad Sci U S A 98:13681-13686

25. Fox T, Coll JT, Xie X, Ford PJ, Germann UA, Porter MD, Pazhanisamy S, Fleming MA, Galullo V, Su MS, Wilson KP 1998 A single amino acid substitution makes ERK2 susceptible to pyridinyl imidazole inhibitors of p38 MAP kinase. Protein Sci 7:2249-2255

26. Waas WF, Lo HH, Dalby KN 2001 The kinetic mechanism of the dual phosphorylation of the ATF2 transcription factor by p38 mitogen-activated protein (MAP) kinase alpha. Implications for signal/response profiles of MAP kinase pathways. J Biol Chem 276:5676-5684

27. Ben Levy R, Hooper S, Wilson R, Paterson HF, Marshall CJ 1998 Nuclear export of the stress-activated protein kinase p38 mediated by its substrate MAPKAP kinase-2. Curr Biol 8:1049-1057

28. Burgering BM, Medema RH, Maassen JA, van de Wetering ML, van der Eb AJ, McCormick F, Bos JL 1991 Insulin stimulation of gene expression mediated by p21ras activation. EMBO J 10:1103-1109

29. van den Berghe N, Ouwens DM, Maassen JA, van Mackelenbergh MG, Sips HC, Krans HM 1994 Activation of the Ras/mitogen-activated protein kinase signaling pathway alone is not sufficient to induce glucose uptake in 3T3-L1 adipocytes. Mol Cell Biol 14:2372-2377

30. Angel P, Hattori K, Smeal T, Karin M 1988 The jun proto-oncogene is positively autoregulated by its product, Jun/AP-1. Cell 55:875-885

31. Sanders J, Brandsma M, Janssen GM, Dijk J, Moller W 1996 Immunofluorescence studies of human fibroblasts demonstrate the presence of the complex of elongation factor-1 beta gamma delta in the endoplasmic reticulum. J Cell Sci 109:1113-1117

32. Pronk GJ, Vries-Smits AM, Ellis C, Bos JL 1993 Complex formation between the p21ras GTPase-activating protein and phosphoproteins p62 and p190 is independent of p21ras signalling. Oncogene 8:2773-2780

**Supplemental figures to Chapter 4**

## S1
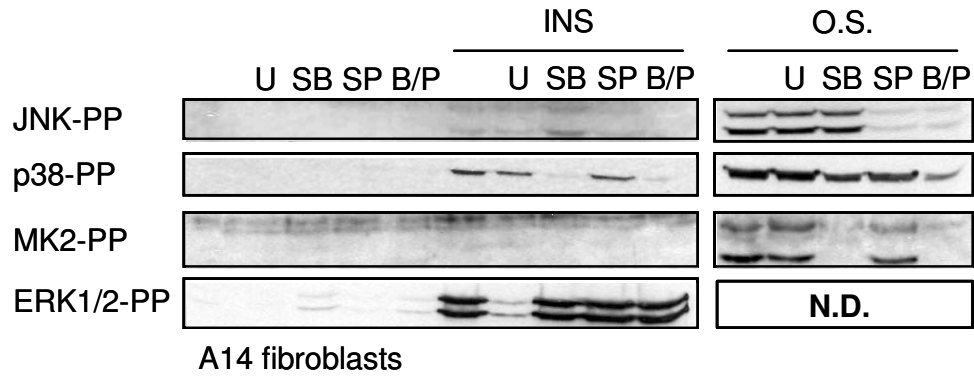


SUPPL. FIG S1. Serum-starved A14 cells were treated with DMSO or 10 µM U0126 (U; 15 minutes), 2.5 µM SB203580 (SB; 30 minutes), 10 µM SP600125 (SP; 30 minutes) or SB and SP (B/P; 30 minutes) prior to 15 minute-treatments with 10 nM insulin (INS) or osmotic shock (O.S.; 0.5M NaCl). Cell lysates were prepared and analyzed with antibodies specific for phosphorylated JNK, p38, MAPKAPK2 (MK2) and ERK. N.D. is not determined.

## S2
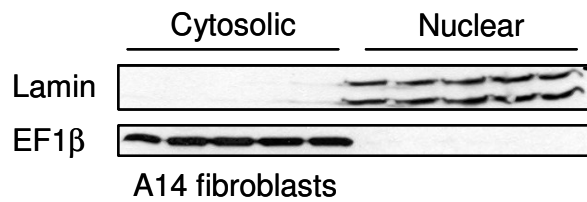


SUPPL. FIG. S2. Crude cell fractions were prepared from serum-starved, insulin-stimulated A14 fibroblasts as described in Materials and Methods. Cytosolic and nuclear fractions were immunoblotted using EF-1β and Lamin A antibodies as cytosolic and nuclear markers, respectively. No cytosolic leak could be detected in the nuclear pellets used for protein extraction.